



Final report

**Analysis of the Physical Interaction between Fas–Associated
Death Domain (FADD) and Tripartite Motif-Containing 21
(Trim21), an E3 Ubiquitin Ligase**

By

Dr. Decha Sermwittayawong

This work was supported by the 2554-2555 Fiscal Budget Fund

Grant # SCI540034S

Abstract

Fadd and Trim21 interact with each other to negatively regulate IFN- α expression in response to viral infection. However, the physical association between the two proteins is not completely understood. In this study, the interaction between Fadd and Trim21 was reinvestigated. I found that Fadd interacts with Trim21 through the F25 and K33, which are the surface amino acids on Fadd. As for Trim21, both coiled-coil and B30.2 domains are necessary and sufficient for interaction with Fadd. Despite these findings, I was unable to show subcellular colocalization between the two proteins and the effect of Trim21-interaction defective Fadd mutants on Trim21 self-ubiquitination. These experiments to show the functional relationship of the two proteins are technically difficult and probably require a certain experimental condition such as using virus to infect cells.

Fadd และ Trim21 สร้างปฏิสัมพันธ์กันเพื่อต่อต้านการแสดงออกของ IFN- α ในการตอบสนองต่อการติดเชื้อไวรัส อย่างไรก็ตาม ปฏิสัมพันธ์ทางกายภาพระหว่างโปรตีนทั้งสองยังไม่เป็นที่เข้าใจอย่างชัดเจน ในการศึกษาครั้งนี้ ได้ทำวิเคราะห์การปฏิสัมพันธ์ทางกายภาพของโปรตีนทั้งสองอีกครั้ง ซึ่งพบว่า Fadd สร้างปฏิสัมพันธ์กับ Trim21 ผ่านทาง F25 และ K33 ซึ่งเป็นกรดอะมิโนบนผิวของโปรตีน Fadd และสำหรับ Trim21 coiled-coil และ B30.2 โดเมน มีความจำเป็นและเพียงพอต่อการสร้างปฏิสัมพันธ์กับ Fadd ถึงอย่างไรก็ตาม ข้าพเจ้าไม่สามารถแสดงการอยู่ร่วมกันของโปรตีนทั้งสองภายในเซลล์ และไม่สามารถแสดงให้เห็นได้ว่า Fadd mutants ที่ไม่สร้างปฏิสัมพันธ์กับ Trim21 มีผลต่อ คุณสมบัติ self-ubiquitination การทดลองที่แสดงให้เห็นถึงความสัมพันธ์ทางหน้าที่ระหว่างโปรตีนทั้งสองเป็นงานที่ยากทางเทคนิค และอาจจะต้องการเงื่อนไขทางการทดลองบางประการ เช่น การให้ไวรัสเข้าไปบุกรุกเซลล์ เป็นต้น

Table of contents

List of Figures	iv
List of Tables	v
List of Abbreviations	vi
Acknowledgements	vii
Introduction	1
Materials and methods	5
Results	10
Discussion	19
References	21
Appendix A: ECONOMICAL METHOD FOR MIDIPREP PLASMID DNA PURIFICATION USING DIATOMACEOUS EARTH	
Abstract.....	26
Introduction.....	27
Materials and methods.....	28
Results.....	31
Discussion.....	37
References.....	38

List of Figures

Figure 1: F25Y and K33E mutations in Fadd abolished interaction with Trim21...	11
Figure 2: The B30.2 and Coiled-coil domains of Trim21 are required for Fadd interaction.....	13
Figure 3: Fadd and Trim21 do not colocalize within the same compartment.....	15
Figure 4: Fadd mutations that affect Trim21 self-ubiquitination.....	16
Figure 5: Homemade spun column.	31
Figure 6: Percent recovery of the plasmid from different amount of DE.....	32
Figure 7: Hot water is the best solution to elute plasmids from the resin.....	33
Figure 8: Analysis of purified plasmids with agarose gel electrophoresis and transfection assay.....	34

List of Tables

Table 1: Some of the primers used in this study.....	7
Table 2: Relative intensity of unmodified Trim21 from Figure 4.....	16
Table 3: Adjusted percent intensity of all ubiquitinated Trim21 from Figure 4.....	17
Table 4: Absorbances of plasmids purified with this technique.....	35
Table 5: Comparing Qiagen plus midi kit and the homemade spun column.....	36
Table 6: Comparing the cost of purification kits and the homemade spun column..	37

List of Abbreviations

C-FLIP	Cellular FLICE-like inhibitory protein
CC domain	Coiled-coil domain
CoIP	Co-immunoprecipitation
DD	Dead domain
DE	Diatomaceous earth
DED	Death-effector domain
Fadd	Fas-associated death domain
IRF3	Interferon regulatory factor 3
IRF7	Interferon regulatory factor 7
SDM	Site-directed mutagenesis
SDS-PAGE	Sodium Dodecyl Sulfate-Polyacrylamide Gel Electrophoresis
Trim21	Tripartite motif-containing 21

Acknowledgements

This has been a difficult and challenging project and it comprises more failure than success. Nevertheless, I must admit that I have learned a great deal from it. Many people on this list deserve my sincere thank you: Ms. Nureeya Waji, for all helps and hard work; Associate Professor Dr. Nongporn Towatana for everything, including constant supports and advice; Professor Dr. Astar Winoto at the University of California at Berkeley for many Fadd, Trim21, and IRF constructs. Also, I am grateful to all helps and support from the Department of Biochemistry where I work and to the Excellent Center for Genomics and Bioinformatics Research where I started this project there. This research would not be possible without monetary support, mainly from the Fiscal Budget Fund (2554-2555, # SCI540034S) and partly from the Science Achievement Scholarship of Thailand (SAST).

Introduction

Fas-associated death domain (FADD) is an adaptor protein involved in Fas-induced cell apoptosis as well as cell proliferation in T-lymphocytes (Zhang et al. 1998; Zhang et al. 2001; Osborn et al. 2007). Structure of FADD has been determined by NMR spectra (Carrington et al. 2006). FADD consists of two domains: Death-effector domain (DED) and Death domain (DD), and a C-terminal tail, which is subjected to phosphorylation (Hua et al. 2003; Alappat et al. 2005). DED is required for self-interaction and binding with procaspase-8, whereas DD interacts with Fas/Apo1/CD95, a member of the tumor necrosis factor receptor (TNFR) (Carrington et al. 2006). Its interaction with CD95 triggers the formation of Death-inducing signaling complex (DISC) to signal the apoptosis pathway, which involves activation of caspase-8 or 10 (Scaffidi et al. 1999; Roy et al. 2008). In contrast to apoptosis, FADD is also required for a proper T-cell proliferation. Both FADD knock out mice and a S194D point mutation of FADD block T-cells from exiting the G1 phase (Osborn et al. 2007). Clearly, phosphorylation-dephosphorylation of a single serine on the C-terminal tails plays an important role in cell-cycle regulation.

In addition to apoptosis and cell proliferation functions, FADD might play other roles in cells. To test this idea, co-immunoprecipitation was performed to search for additional FADD interacting proteins. Trim21 is one of the proteins co-precipitated with FADD (Young et al. 2011). Tripartite motif-containing 21(Trim21) is a member of Trim Superfamily, which functions in many diverse pathways such as development, cell cycle and immunity (Sabile et al. 2006; Higgs et al. 2008; Yang et al. 2009). Previously known as auto-antigen protein, Trim21 possesses 4 functional domains: Ring, B-box, coiled-coil

(RBCC), and B30.2 domains (Nisole et al. 2005). Biochemical studies suggest that Trim21 is an E3 ubiquitin ligase that can ubiquitinate itself but the significance of Trim21 auto-ubiquitination remains unclear (Wada and Kamitani 2006a; Espinosa et al. 2008). Besides self-ubiquitination, Trim21 also targets many other proteins. These include Interferon Regulatory Factors (IRF) 3, 7, and 8 (Kong et al. 2007; Higgs et al. 2008; Yang et al. 2009), p27^{Kip1} (Sabile et al. 2006), UnpEl/Usp4 (Wada and Kamitani 2006b), IgG (Takahata et al. 2008), and Trim5 (Diaz-Griffero et al. 2006). Thus, it is increasingly clear that Trim21 is involved many functions in cells.

Fadd and Trim21 function to regulate the expression of type I interferon through the IRF proteins (Young et al. 2011). It has been shown by many investigators that Trim21 ubiquitinates IRF3 and IRF7 (Higgs et al. 2008; Yoshimi et al. 2009; Young et al. 2011). The ubiquitinated IRF proteins are targeted to proteasomal degradation, causing a decrease in the production of type I interferons (Higgs et al. 2008; Higgs et al. 2010). Young and colleagues showed that overexpression of Fadd enhanced Trim21 auto-ubiquitination, which correlated with the increase in the overall ubiquitination of IRF7 and the decrease in the production of interferon- α (IFN- α) (Young et al. 2011). The investigators also showed that Fadd utilized the DED to interact with Trim21, and a deletion of the C-terminal B30.2 domain of Trim21 abolished the association with Fadd. In addition, the D74A mutation in the DED of Fadd somewhat affected but not totally diminished Trim21 interaction.

Although the physical interaction between Fadd and Trim21 has been suggested in details, the comprehensive knowledge of how they associate with each other is yet to be understood. First, the specific D74A mutation in Fadd did not completely fail to

interact with Trim21 (Young et al. 2011). It has been shown that this residue is part of a conserved motif RXDLL found in many DED containing proteins such as Fadd, Caspase-8, and cellular FLICE-like inhibitory protein (C-FLIP) (Muppidi et al. 2006). This conserved RXDLL motif was shown to mediate protein-protein interaction (Hill et al. 2002; Muppidi et al. 2006). However, NMR spectroscopy suggested that the D74A mutation in hFadd caused a dynamic structural disorder in the DED (Carrington et al. 2006), and this might explain the partial loss of the interaction between the mutant Fadd and Trim21 (Young et al. 2011). Second, Young et al showed that Fadd did not interact with the C-terminally truncated Trim21 (Young et al. 2011), suggesting that the B30.2 domain on the C-terminal of Trim21 is required for Fadd interaction. While the DED of Fadd was shown to be necessary and sufficient with Trim21 interaction (Young et al. 2011), it is not clear whether the B30.2 domain of Trim21 itself is sufficient for its interaction with Fadd because other domains in Trim21 might also be required for Fadd-Trim21 association.

Asides from how Fadd and Trim21 interact with one another, subcellular localization of both proteins is quite interesting—both of them were reported to be in both nuclear and cytosolic fractions. Fadd must reside in the cytosol in order to function in the Fas-induced cell apoptosis (Kischkel et al. 1995; Scaffidi et al. 1999). However, Fadd can also be shuffled into the nucleus to regulate cell cycle progression (Alappat et al. 2003; Alappat et al. 2005). In addition, the immunofluorescence staining and GFP fusion Fadd experiments also suggest nuclear localization of this protein (Gomez-Angelats and Cidlowski 2003; Frisch 2004). It might be possible that nuclear localization of Fadd protects cells from undergoing cell apoptosis, or Fadd is translocated into cytosol

when cell receives an apoptotic signal. In contrast to Fadd, Trim21 mainly localizes in the cytosol (Keech et al. 1995; Ohlsson et al. 2002). Interestingly, nuclear translocation of Trim21 happened when cells were exposed to nitric oxide (Espinosa et al. 2008). In addition, Trim21 was induced by IFN- α and translocated into the nucleus (Strandberg et al. 2008). Therefore, it seems that Trim21 is preferred to be in cytosol, whereas Fadd is mainly found in the nucleus. It would be interesting to see if co-expression of Fadd and Trim21 would change the preference of subcellular localization of each protein.

In this work, physical interaction between Fadd and Trim21 was reinvestigated. I found that the F25 and K33 surface residues of Fadd are required for the interaction with Trim21. The B30.2 domain of Trim21 is necessary but not sufficient for interaction with Fadd protein. In order for Trim21 to interact with Fadd, both coiled-coil (CC) and the B30.2 domains must be present. Surprisingly, Fadd and Trim21 do not co-localize within the same cellular compartment: Fadd is present in the nucleus, whereas Trim21 is localized in the cytosol. Based on this study, it is not clear whether Fadd enhances Trim21 self-ubiquitination since the F25Y but not the K33E Fadd mutant showed a decrease in the overall ubiquitinated Trim21. The interaction between Fadd and Trim21 is more difficult and complicated than previously thought. Perhaps, a certain experimental condition such as viral infection may be required to illustrate a functional relationship between the two proteins.

Materials and methods

Plasmids and cloning strategies

Three mammalian expression plasmids: pCI, pCI-hFaddHisFlag, pCI-hFaddHisFlag D74A, pCI-hFaddHisFlag K33E, pcDNA3-HAhTrim21, and pCI-hTrim21 were kindly given by Prof. Dr. Astar Winoto at the University of California at Berkeley. Additional plasmids: pCI-HA, pCI-HAhTrim21 Δ 1 (275-475), and pCI-HAhTrim21 Δ 3 (131-475), pCI-HAhTrim21 Δ 4 (131-275), and pCI-HAhTrim21 Δ 5 (183-275) were created in this work. Short affinity tags such as the 6xHistidine (His) tag, *Strep* tag-II (STR) tag (NH₂-WSHPQFEK-COOH), Flag tag (NH₂-DYKDDDDK-COOH) and the Hemagglutinin (HA) tag (NH₂-YPYDVPDYA-COOH) are chosen because they are less likely to interfere with protein folding (Lichty et al. 2005). To create pCI-HA plasmid, the annealed oligo primers for the N-terminal HA tag was cloned into the vector, using NheI and EcoRI restriction sites. To create pCI-HAhTrim21 Δ 1, the hTrim21 Δ 1 fragment created with polymerase chain reaction (PCR) was subcloned into the pCI-HA vector, using EcoRI and KpnI restriction sites. Other plasmids: pCI-HAhTrim21 Δ 3, pCI-HAhTrim21 Δ 4, and pCI-HAhTrim21 Δ 5 were also created in the same manner. Primers used for creating plasmids in this study are listed in Table 1.

Site-directed mutagenesis

Site-directed mutagenesis (SDM) was used to mutate the specific residue in the gene. These following plasmids: pCI-hFaddHisFlag S18A, pCI-hFaddHisFlag E22A, pCI-hFaddHisFlag L28E, pCI-hFaddHisFlag F25Y, pCI-hFaddHisFlag R34E, pCI-hFaddHisFlag K35E, pCI-hFaddHisFlag R71E, and pCI-hFaddHisFlag H73A were created in this work. SDM was performed using QuikChange based mutagenesis

protocol (Stratagene). Primers used for site-directed mutagenesis (SDM) are provided in Table A1. Once a certain construct is mutated, the mutated gene was sequenced to confirm the absence of any unwanted mutation, even if high-fidelity DNA polymerases were used.

Cell culture and condition

HEK293T cells (ATCC: CRL 11268) was purchased from the ATCC and used for transfection assay. This cell line was maintained with the Dulbecco's Modified Eagle's Medium (DMEM) supplemented with 10% fetal bovine serum (FBS) and propagated at 37°C incubator with 5% CO₂.

Transfection assay

Both Trim21 and Fadd plasmids were co-transfected into the cells using Lipofectamine 2000 (Invitrogen) or Trans LT1 (Mirus) as recommended by the manufacturer's instruction. Transfected cells were collected 48 hours post transfection.

Co-immunoprecipitation assay

Co-immunoprecipitation (CoIP) assay was used for testing Fadd-Trim21 interaction. Briefly, cells were lysed with the lysis buffer (50 mM Tris-Cl pH 7.4, 150 mM NaCl, 1 mM EDTA, 0.5 % NP-40, 10% glycerol, 1 mM NaF, 1 mM Na₃VO₄, and 1x Protease Inhibitor from Roche) and centrifuged at 13000 rpm for 60 minutes at 4°C. A small amount of lysate was collected for Western blot analysis and the remaining extract was incubated with 10 µg anti-Flag tag monoclonal antibody (Sigma) for 2 hours. Then, the protein-antibody complex was incubated with Protein A agarose beads (Pierce) for another one hour. After incubation, the supernatant was collected and washed with wash buffer (50 mM Tris-Cl pH 7.4, 150 mM NaCl, 1 mM EDTA, 0.5 % NP-40, and 10%

glycerol). Proteins in both lysates and bead fractions were fractionated with SDS-PAGE and evidence of interaction was analyzed through Western blotting.

Table 1: Some of the primers used in this study

Construct/ mutation	Forward primer	Reverse primer
HA tag	CTAGCGCCACCATGTACCCATATG ACGTCCCAGATTACGCAG	AATTCTGCGTAATCTGGGACGTCAT ATGGGTACATGGTGGCG
hTrim21Δ1	GCGAATTCGGGCTGAAGAAGATGC TGA	CCGGTACCTCAATAGTCAGTGGAT CCTTG
hTrim21Δ3	GCGAATTCGCTGCACAGGAGTACC	CCGGTACCTCAATAGTCAGTGGAT CCTTG
hTrim21Δ4	GCGAATTCGCTGCACAGGAGTACC	GCGGTACCTTATGGCACATGGCAC ACA
hTrim21Δ5	GCGAATTCGTGCAGCAAAAAAACT TCCTG	GCGGTACCTTATGGCACATGGCAC ACA
hFadd (L28E)	AAGTTCCTATGCGAGGGGCGCGTG GGC	GCCACGCGCCCCTCGCATAGGAA CTT
hFadd (K33E)	TCGGGCGCGTGCGGAGCGCAAGC TGGA	TCCAGCTTGCCTCGCCACGCGC CCGA
hFadd (R34E)	CGCGTGGGCAAGGAGAAGCTGGAG CGCGTG	CACGCGCTCCAGCTTCTCCTTGCCC ACGCG
hFadd (K35E)	TGGGCAAGCGCGAGCTGGAGCGC	GCGCTCCAGCTCGCGCTTGCCCA
hFadd (D44R)	AGAGCGGCCTACGCCTCTTCTCC	GGAGAAGAGGCGTAGGCCGCTCT
hFadd (F25Y)	CGAGCTCAAGTACCTATGCCTCG	CGAGGCATAGGTACTTGAGCTCG
hFadd (E22A)	AGCGAGCTGACCGCGCTCAAGTTC CTA	TAGGAACTTGAGCGCGGTCAGCTC GCT
hFadd (S18A)	AGCCTGTCGAGCGCCGAGCTGACC GA	TCGGTCAGCTCGGCGCTCGACAGG CT
hFadd (R71E)	CTCGCCTCCCTGGAGCGCCACGAC CTGC	GCAGGTCGTGGCGCTCCAGGGAGG CGAG
hFadd (H73A)	CCCTGCGGCGCGCCGACCTGCTGC GG	CCGCAGCAGGTCGGCGCGCCGAG GG

Western blotting

The identity of the protein at the expected molecular weight can be confirmed by Western blotting assay. All steps were performed at room temperature unless indicated. Briefly, after performing SDS-PAGE, proteins on the gel were transferred to nitrocellulose membrane (Bio-Rad). Proteins on the membrane can be visualized by

staining with 0.2% Ponceau Red in 10% acetic acid and destained with distilled water. Subsequently, the membrane was blocked with blocking solution (5% non-fat milk in 1xTBST, which contains 0.025 M Tris-Cl pH 8.0, 150 mM NaCl, and 0.05% Tween 20) for 1 hour with constant rocking. The membrane was washed 3x 5 min with 1x TBST and incubated with 10 ml 1:1000 diluted anti-His tag monoclonal antibody (GE Healthcare) for 1 hour using the same incubation condition. The membrane was then washed with 1xTBST for 3 times, 5 minutes interval before subjected to a 1-hour incubation with an anti-mouse HRP conjugated secondary antibodies (GE Healthcare) diluted 1:5000 with 1xTBST. Subsequently, the membrane was washed 3x 5 minutes with 1x TBST before adding SuperSignal West Pico Chemiluminescent Substrate (Pierce) and exposed to an X-ray films (Pierce) at various time. X-ray film was developed.

Nuclear vs cytosolic extraction

To perform nuclear and cytosolic extractions, freshly harvested cells must be used. All steps were performed at 4°C, unless indicated otherwise. After 48-hour post transfection, cells were collected by trypsinization and the pellet was resuspended in 275 µl buffer A (10 mM Hepes pH 7.9, 1 mM KCl, 0.1 mM EDTA, 0.5% NP-40, 1 mM DTT, 1x complete set protease Inhibitor (Roche), and 1 mM PMSF). Cells were allowed to swell on ice for 5 minutes and 25 µl was saved for the “whole” fraction. Then, the nuclear pellet was precipitated by centrifugation at 850 x g for 5 minutes. The resulting supernatant, which is the cytosolic extract, was transferred to a clean tube. Then, the pellet was washed trice with 1 ml buffer A without NP-40 and centrifuged at the same speed for 1 minute. After washing, the nuclear pellet was resuspended with 250 µl buffer C (20 mM Hepes pH 7.9, 0.4 M NaCl, 1 mM EDTA, 1 mM DTT, and 1 mM PMSF) and

rotated for 30 minutes. Cellular and nuclear debris were separated by centrifugation at 16,060 x g for 10 minutes and the supernatant is the nuclear extract. Proteins in the whole, cytosolic, and nuclear fractions were fractionated by SDS-PAGE and subjected to Western blotting analysis using the appropriate antibodies.

Results

Mutations in Fadd that affect interaction with Trim21

In order to search for Fadd mutations that affect interaction with Trim21 proteins, a number of Fadd mutants were created through SDM, and the interaction between Fadd mutants and wild-type Trim21 proteins was analyzed. SDM was performed only on some of the surface residues of the DED since mutations on those residues are less likely to affect the 3D structure of the protein. In addition, the NMR structure of the DED of Fadd has previously determined (Carrington et al. 2006), allowing the identification of surface residues of DED.

The sites of point mutations in Fadd could be divided into two groups. First group is the surface residues around the D74 since the D74A Fadd mutant was previously shown to attenuate the interaction with Trim21 (Young et al. 2011). Second group of point mutations clusters around the F25 since the tyrosine amino acid substitution at this residue (F25Y) blocked protein aggregation *in vitro* (Eberstadt et al. 1998; Carrington et al. 2006). Thus, several Fadd mutants, including S18A, E22A, L28E, F25Y, R34E, K35E, R71E, and H73A were created. Among these mutations, the F25Y and the K33E mutations in Fadd totally disrupted the interaction with Trim21 (Figure 1). The defect in interaction with Trim21 observed in those Fadd mutants was not due to the folding problem since the F25Y, E22A, and K33E Fadd mutant proteins are highly soluble compared with the wild type protein (data not shown). In addition, the R34E and D74A Fadd mutants could weakly interact with Trim21 (Figure 1).

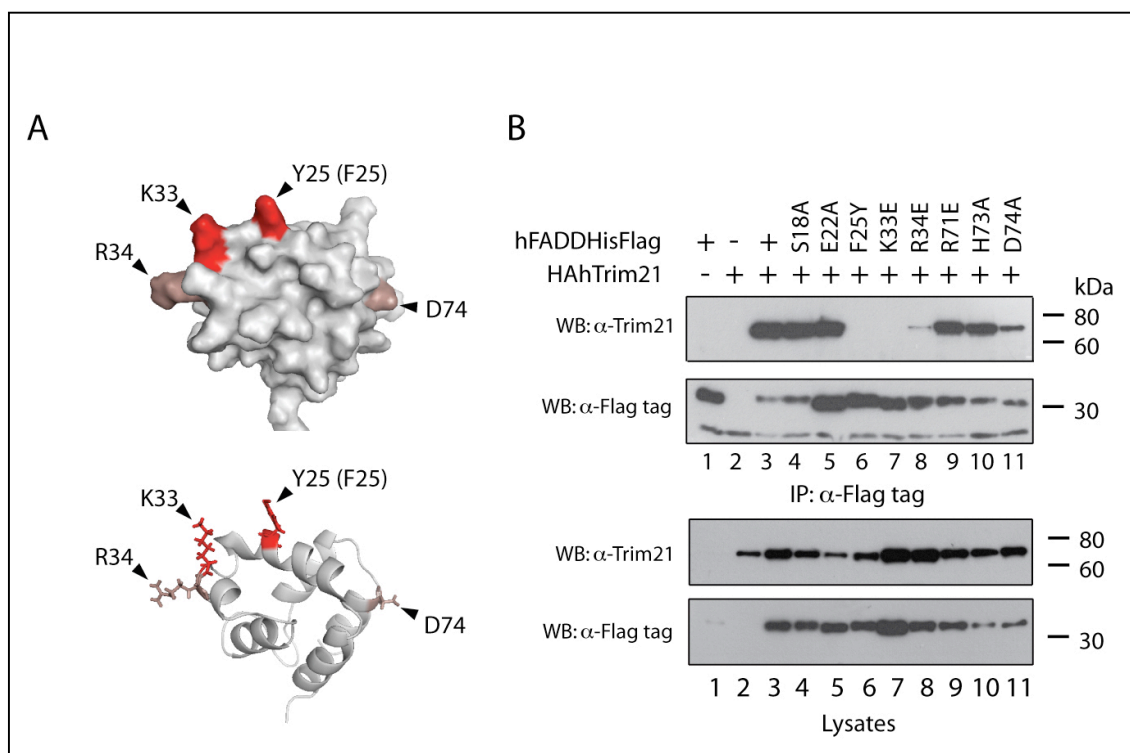


Figure 1: F25Y and K33E mutations in Fadd abolished interaction with Trim21. A) A cartoon of the DED of Fadd protein shows the residues that are required for Trim21 interaction. Red amino acids are critical for Trim21 interaction whereas the residues in the darksalmon color are somewhat required for such interaction. B) Flag IP between Flag-tagged Fadd and HA-tagged Trim21. Trim21 protein cannot coprecipitate with Flag-tagged F25Y and K33E Fadd mutants

The residues F25, K33, and L28 on the DED of Fadd were shown to play important role in self-association, interaction with CD95 receptor, and with Caspase-8 (Carrington et al. 2006; Sandu et al. 2006). However, the L28E mutation in Fadd did not interfere with Trim21 interaction (data not shown), suggesting that Trim21-Fadd interaction is independent of Fadd-Fadd interaction. Noticed that the F25 and K33 are not on the same helices but positioned very closed together in the structure (Figure 1A). Although the R34 is a consecutive residue to the K33, the arginine side chain points away from the surface of K33 and F25 (Figure 1A). The direction of the arginine side chain probably explains the partial effect of the R34E mutation on Trim21 interaction. The

D74A mutation on Fadd also displayed some partial effect on Trim21 interaction (Figure 1B); however, this residue is not on the same cluster as F25, K33, and R34 (Figure 1A). In addition, the D44R mutation in Fadd disrupted the interaction of the mutant Fadd with Caspase-8 (Sandu et al. 2006) but not with Trim21 (data not shown). Therefore, it is possible that Fadd interacts with Trim21 but not together with Caspase-8 at the same time.

The B30.2 domain is not sufficient to support interaction with Fadd

The analysis on Trim21 was mainly focused on the role of specific domains, rather than the role of specific residues as done with Fadd. Thus, the major question regarding Trim21 is whether the B30.2 domain by itself would be sufficient for interaction with Fadd. To do this, several Trim21 truncation constructs were created, and the interaction of each truncated Trim21 was analyzed by co-immunoprecipitation assay. Results in Figure 2 show that Trim21 Δ 1 (275-475), which contains only the B30.2 domain was not able to interact with Fadd, (Figure 2B lane 10 and 2C lane 11), suggesting that this domain by itself is not sufficient to physically associate with Fadd protein. However, when the coiled-coil domain (CC domain) is present, the polypeptide (Trim21 Δ 3) was able to co-immunoprecipitate with Fadd (Figure 2B lane 9 and 2C lane 12), indicating that the CC domain might facilitate the interaction with Fadd protein. To test the role of CC domain, the two additional truncations of Trim21: Trim21 Δ 4 (131-275) and Trim21 Δ 5 (183-275) were created and used for co-immunoprecipitation. The results show that these polypeptides of Trim21 could not associate with Fadd (Figure 2C lanes 13 and 14). Together, these results suggest that both the B30.2 and the CC domains but not each of them alone are required for the physical association of Trim21 with Fadd.

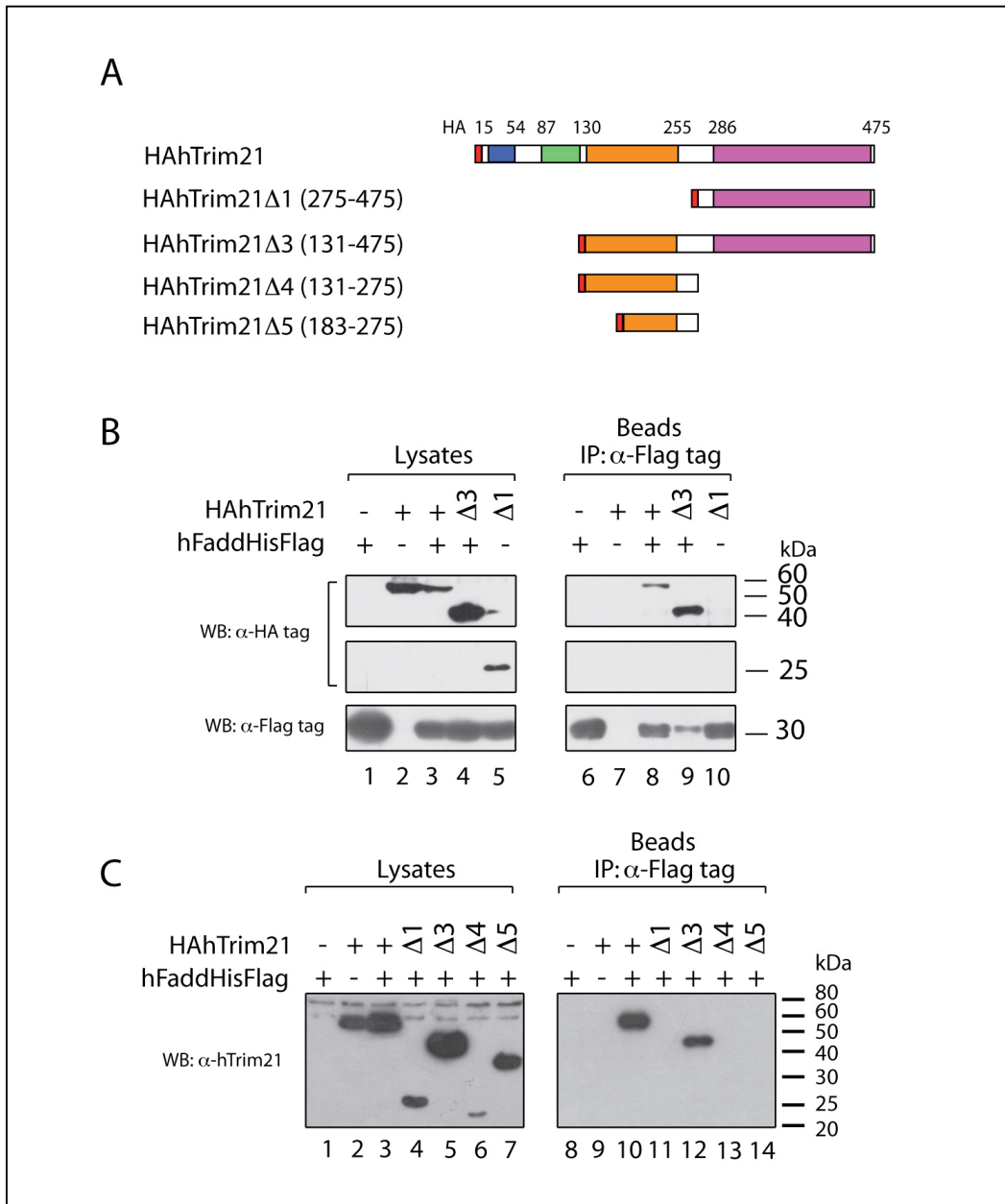


Figure 2: The B30.2 and Coiled-coil domains of Trim21 are required for Fadd interaction. A) Cartoons illustrate truncated Trim21 proteins that were used in the CoIP assay. B) CoIP between wild type, Trim21 $\Delta 1$, and Trim21 $\Delta 3$ and Fadd. Only the wild type and Trim21 $\Delta 3$ were able to interact with Fadd. C) Same as B) except that the experiment was performed separately and with two additional Trim21 truncations: Trim21 $\Delta 4$ and Trim21 $\Delta 5$.

The CC domain has been shown to promote protein dimerization and oligomerization of Trim proteins (Niikura et al. 2003; Stremlau et al. 2006). Trim21 was shown to form a stable dimer *in vitro*, and the dimerization requires the CC domain (Mallery et al. 2010). To investigate whether Trim21 dimerization is required for Fadd interaction, the CC domain of Trim21 was replaced with the CC domain from yeast Gcn4 (yCCG). This CC domain exists as a parallel dimer of leucine zipper in the X-ray crystal structure (O'Shea et al. 1991). The interaction between the chimeric yCCG-B30.2 and Fadd was analyzed by co-immunoprecipitation assay. However, it failed to immunoprecipitate Fadd (data not shown). One possible interpretation is that some of the residues in the CC domain of Trim21 might also interact with Fadd. Another possibility is that the Trim21 dimerization is not involved in Trim21-Fadd interaction, but the CC domain might contribute to the overall stability of the B30.2 domain for proper interaction with Fadd. Regardless of these interpretations, additional experiments are required to address the role of the Both CC and B30.2 domains in Fadd interaction.

Fadd and Trim21 do not co-localize within the same cellular compartment

The interaction between Fadd and Trim21 observed in the co-immunoprecipitation experiment suggests that the two proteins might reside within the same cellular compartment. To investigate this possibility, cytosolic and nuclear fractions isolated from cells co-transfected with Fadd and Trim21 expressing plasmids were used to analyze the presence of both proteins. The results show that Fadd remained in the nucleus, whereas Trim21 was found in the cytosol (Figure 3 left panel).

Trim21 and Fadd play an important role in viral infection. For example, Fadd is required for Fas-induced cell apoptosis upon viral infection (Balachandran et al. 2000).

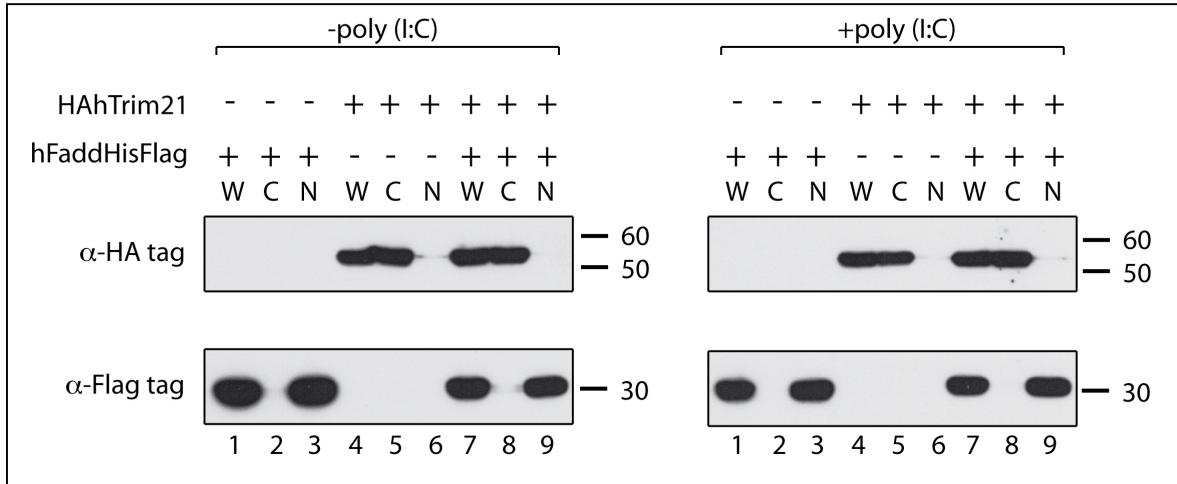


Figure 3: Fadd and Trim21 do not colocalize within the same compartment. Plasmids encoded for Flag-tagged Fadd and HA-tagged Trim21 were transfected into HEK293T cells. Extraction of nuclear (N) and cytosolic (C) components was performed and compared with the whole cell (W). Left and right panels, the transfection experiments were performed without and with poly (I:C), respectively. Western blotting with anti-Flag tag and anti-HA tag antibodies suggests that Fadd is mainly localized within the nucleus, whereas Trim21 resides within the cytosolic compartment.

In addition, Fadd interacts with Trim21 to enhance Trim21 self-ubiquitination activity to ubiquitinate IRF7, leading to down-regulation of IFN- α expression (Young et al. 2011). The relationship between Fadd and Trim21 suggests that colocalization of both proteins might be observed when cells were infected with virus, especially the Sendai virus (Young et al., 2011). However, viral infection assay cannot be performed in my laboratory due to the lack of reagents, equipments, and the facility. Thus, poly (I:C), a double strand RNA analog was used to mimic viral infection into the cells. The experiment was performed by co-transfecting Trim21 and Fadd expressing plasmids with or without poly (I:C). The localization of the two proteins in cytosol and nucleus were analyzed by mean of Western blotting. Surprisingly, the location of the two proteins were unaffected whether or not poly (I:C) was included: Fadd remained exclusively in the nucleus, whereas Trim21 was found in the cytosol (Figure 3). These results could be

interpreted that the experiment with poly (I:C) was not working, or poly (I:C) could not induce colocalization of Fadd and Trim21.

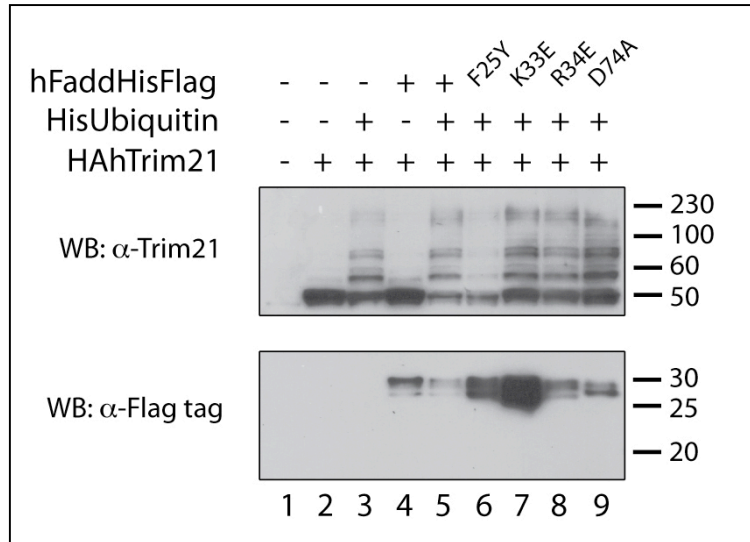


Figure 4: Fadd mutations that affect Trim21 self-ubiquitination. 293T cells were transfected with combinations of plasmid indicated above. Soluble extract of the cells were used for Western blotting analysis with anti-Trim21 and anti-Flag tag for the presence of Trim21 and Fadd, respectively.

Table 2: Relative intensity of unmodified Trim21 from Figure 4

Unmodified Trim21				
Lane	Area (arbitrary unit)	Percent	Relative intensity	Multiplying factor
1	N/D ¹	N/D	N/D	N/D
2	35185.7	15.4	1.0	1.00
3	29334.9	12.8	0.8	1.20
4	36960.8	16.2	1.1	0.95
5	18318.1	8.0	0.5	1.92
6	18387.5	8.0	0.5	1.91
7	30251.4	13.2	0.9	1.16
8	27236.4	11.9	0.8	1.29
9	33119.4	14.5	0.9	1.06

¹ Not determined

Table 3: Adjusted percent intensity of all ubiquitinated Trim21 from Figure 4

Ubiquitinated Trim21				
Lane	Area (arbitrary unit)	Percent	Multiplying factor (from unmodified Trim21)	Adjusted percent intensity
1	N/D ²	N/D	N/D	N/D
2	8539.7	2.7	1.00	2.7
3	36370.8	11.6	1.20	13.9
4	15749.0	5.0	0.95	4.8
5	38129.4	12.2	1.92	23.3
6	17821.1	5.7	1.91	10.9
7	62870.4	20.0	1.16	23.3
8	55745.2	17.8	1.29	23.0
9	78550.8	25.0	1.06	26.6

Fadd mutations that affect Trim21 self-ubiquitination

Trim21 interaction defective Fadd mutants (F25Y, K33E, R34E, and D74A) were used to test their effects on Trim21 self-ubiquitination property. Combinations of Fadd, Trim21, and ubiquitin expression plasmids were co-transfected into 293T cells. The expression of Fadd and Trim21 in the soluble extracts was analyzed by Western blotting on using anti-Trim21 and anti-Fadd antibodies. If Trim21 is ubiquitinated, higher molecular weight bands above Trim21 will result in the Western blot probed with anti-Trim21. Based on the previous study, ubiquitinated Trim21 appeared in the Western blot when a ubiquitin-expressing plasmid was co-transfected, and further enhanced with Fadd-expressing plasmid was also added (Young et al. 2011). The level of ubiquitinated Trim21 among different lanes can be compared if the amount of unmodified Trim21 in each lane is equivalent. However, the level of unubiquitinated Trim21 in Figure 4A was not comparable, and this was not due to the loading problem (data not shown). Using ImageJ software, the intensity of ubiquitinated and unubiquitinated Trim21 in each lane

² Not determined

was measured (Tables 2 and 3, respectively). The intensity of ubiquitinated Trim21 was adjusted according to the intensity of unubiquitinated band, using Trim21 in lane 2 as a reference. Table 3 shows the adjusted percent intensity of ubiquitinated Trim21 in each lane. Consistent with the previous study by Young and colleagues, Trim21 self-ubiquitination was enhanced in the present of both ubiquitin and Fadd (Table 3, lanes 4 and 5). In addition, ubiquitinated Trim21 was greatly reduced when the F25Y Fadd mutant was coexpressed (Table 3, lane 5). However, the modified Trim21 was not affected with the K33E and R34E Fadd mutants, and appeared slightly enhanced with the D74A Fadd mutant (lanes 6-9). These results were in conflict with the co-immunoprecipitation data in Figure 1 and the previous study by Young and colleagues in which the D74A Fadd mutant decreased the overall Trim21 self-ubiquitination.

The inconsistency of the data made it impossible to conclude the effect of Fadd interaction with Trim21. In addition, the discrepancy between the results in Figure 4 and the published data by Young et al suggests that some experimental adjustments are needed. This experiment was repeated and the same results were observed. However, due to a limited resource and time, the relationship between Fadd mutant and Trim21 ubiquitination was not further pursued.

Discussion

The analysis on Fadd-Trim21 physical association was quite challenging. The bacterial expression system was initially the preferred method. However, the bacterial system could not support the expression of soluble full-length Fadd and Trim21. Thus, I inevitably came to a conclusion that the system is not appropriate, and the mammalian expression system must be employed. With the mammalian expression, I tried to investigate the interaction using GST and STR tags for pull down assays. However, the GST-tagged Trim21 (GSThTrim2) could not pull down Fadd, whereas the C-terminal STR-tagged Fadd (hFaddHisSTR) could not interact with Trim21 in a *Strep*-Tactin pull down assay (data not shown). Because of the failure, the strategy was changed to co-immunoprecipitation assay using anti-Flag tag antibody and the Flag-tagged Fadd (hFaddHisFlag) to investigate the physical interaction of Fadd and Trim21. Using this technique, I was able to show that the two residues: F25 and K33 on the DED of Fadd are required for interaction with Trim21. Furthermore, the B30.2 domain of Trim21 is necessary but not sufficient for its interaction with Fadd. The preceding CC domain of Trim21 is required for Trim21 to interact with Fadd.

In addition to the physical interaction, the functional relationship between Fadd and Trim21 were difficult to analyze. First, Trim21 was shown to interact with a number of factors, including IRF3 and IRF7 (Higgs et al. 2008; Yang et al. 2009; Higgs et al. 2010; Young et al. 2011). It was also shown that a deletion of Trim21 affected the overall ubiquitination of IRF3 (Yoshimi et al. 2009). These findings led to an investigation for a possibility that Fadd might affect the interaction between Trim21 and IRF3/IRF7. However, I was not able to show the interaction between Trim21 and

IRF3/IRF7 under GST pull down assay (data not shown), and the presence of IRF3 did not affect the interaction between Fadd and Trim21 in the co-immunoprecipitation assay (data not shown). Thus, the interaction of Fadd-Trim21-IRF3/IRF7 was not further pursued. Second, Fadd and Trim21 were not co-localized within the same compartment. This could be a failure of transfecting poly (I:C) into the cells, or poly (I:C) is not the appropriate agent to show colocalization of the two proteins. Successful analysis for the function of Fadd and Trim21 was performed using RNA virus (Young et al. 2011). Thus, viral infection assay might be a key experiment to illustrate colocalization of Trim21 and Fadd. However, those experiments pose many difficulties and require substantial amount of resources. Third, based on my results, it is not yet clear whether Fadd interaction enhances Trim21 self-ubiquitination. Fadd probably affects Trim21 self-ubiquitination but more troubleshooting on the experimental conditions is required.

In conclusion, the analysis of the interaction between Fadd and Trim21 were not successful. Many more experiments are needed for a comprehensive understanding of Fadd and Trim21 interaction and their biological significances. For example, it will be interesting to determine how Trim21 interacts with Fadd. SDM on surface residues of Trim21 can be performed and the interaction between Trim21 mutants and Fadd could be analyzed through the co-immunoprecipitation assay. Because Fadd could affect Trim21 activity, it will be interesting to test if Fadd-interaction defective Trim21 mutants would affect the self-ubiquitination activity. In addition, the analysis of how Fadd affect Trim21 interaction with other proteins would potentially lead to a function of Trim21 and Fadd beyond the innate immunity.

References

- Alappat, E.C., Feig, C., Boyerinas, B., Volkland, J., Samuels, M., Murmann, A.E., Thorburn, A., Kidd, V.J., Slaughter, C.A., Osborn, S.L. et al. 2005. Phosphorylation of FADD at serine 194 by CKI α regulates its nonapoptotic activities. *Molecular cell* **19**(3): 321-332.
- Alappat, E.C., Volkland, J., and Peter, M.E. 2003. Cell cycle effects by C-FADD depend on its C-terminal phosphorylation site. *The Journal of biological chemistry* **278**(43): 41585-41588.
- Balachandran, S., Roberts, P.C., Kipperman, T., Bhalla, K.N., Compans, R.W., Archer, D.R., and Barber, G.N. 2000. Alpha/beta interferons potentiate virus-induced apoptosis through activation of the FADD/Caspase-8 death signaling pathway. *J Virol* **74**(3): 1513-1523.
- Carrington, P.E., Sandu, C., Wei, Y., Hill, J.M., Morisawa, G., Huang, T., Gavathiotis, E., and Werner, M.H. 2006. The structure of FADD and its mode of interaction with procaspase-8. *Molecular cell* **22**(5): 599-610.
- Diaz-Griffero, F., Li, X., Javanbakht, H., Song, B., Welikala, S., Stremlau, M., and Sodroski, J. 2006. Rapid turnover and polyubiquitylation of the retroviral restriction factor TRIM5. *Virology* **349**(2): 300-315.
- Eberstadt, M., Huang, B., Chen, Z., Meadows, R.P., Ng, S.C., Zheng, L., Lenardo, M.J., and Fesik, S.W. 1998. NMR structure and mutagenesis of the FADD (Mort1) death-effector domain. *Nature* **392**(6679): 941-945.
- Espinosa, A., Oke, V., Elfving, A., Nyberg, F., Covacu, R., and Wahren-Herlenius, M. 2008. The autoantigen Ro52 is an E3 ligase resident in the cytoplasm but enters the nucleus upon cellular exposure to nitric oxide. *Experimental cell research* **314**(20): 3605-3613.
- Frisch, S. 2004. Nuclear localization of FADD protein. *Cell Death Differ* **11**(12): 1361-1362; author reply 1362-1364.
- Gomez-Angelats, M. and Cidlowski, J.A. 2003. Molecular evidence for the nuclear localization of FADD. *Cell Death Differ* **10**(7): 791-797.
- Higgs, R., Lazzari, E., Wynne, C., Ni Gabhann, J., Espinosa, A., Wahren-Herlenius, M., and Jefferies, C.A. 2010. Self protection from anti-viral responses--Ro52 promotes degradation of the transcription factor IRF7 downstream of the viral Toll-Like receptors. *PLoS One* **5**(7): e11776.
- Higgs, R., Ni Gabhann, J., Ben Larbi, N., Breen, E.P., Fitzgerald, K.A., and Jefferies, C.A. 2008. The E3 ubiquitin ligase Ro52 negatively regulates IFN-beta

- production post-pathogen recognition by polyubiquitin-mediated degradation of IRF3. *J Immunol* **181**(3): 1780-1786.
- Hill, J.M., Vaidyanathan, H., Ramos, J.W., Ginsberg, M.H., and Werner, M.H. 2002. Recognition of ERK MAP kinase by PEA-15 reveals a common docking site within the death domain and death effector domain. *EMBO J* **21**(23): 6494-6504.
- Hua, Z.C., Sohn, S.J., Kang, C., Cado, D., and Winoto, A. 2003. A function of Fas-associated death domain protein in cell cycle progression localized to a single amino acid at its C-terminal region. *Immunity* **18**(4): 513-521.
- Keech, C.L., Gordon, T.P., and McCluskey, J. 1995. Cytoplasmic accumulation of the 52 kDa Ro/SS-A nuclear autoantigen in transfected cell lines. *J Autoimmun* **8**(5): 699-712.
- Kischkel, F.C., Hellbardt, S., Behrmann, I., Germer, M., Pawlita, M., Krammer, P.H., and Peter, M.E. 1995. Cytotoxicity-dependent APO-1 (Fas/CD95)-associated proteins form a death-inducing signaling complex (DISC) with the receptor. *EMBO J* **14**(22): 5579-5588.
- Kong, H.J., Anderson, D.E., Lee, C.H., Jang, M.K., Tamura, T., Tailor, P., Cho, H.K., Cheong, J., Xiong, H., Morse, H.C., 3rd et al. 2007. Cutting edge: autoantigen Ro52 is an interferon inducible E3 ligase that ubiquitinates IRF-8 and enhances cytokine expression in macrophages. *J Immunol* **179**(1): 26-30.
- Lichty, J.J., Malecki, J.L., Agnew, H.D., Michelson-Horowitz, D.J., and Tan, S. 2005. Comparison of affinity tags for protein purification. *Protein Expr Purif* **41**(1): 98-105.
- Mallery, D.L., McEwan, W.A., Bidgood, S.R., Towers, G.J., Johnson, C.M., and James, L.C. 2010. Antibodies mediate intracellular immunity through tripartite motif-containing 21 (TRIM21). *Proc Natl Acad Sci U S A* **107**(46): 19985-19990.
- Muppidi, J.R., Lobito, A.A., Ramaswamy, M., Yang, J.K., Wang, L., Wu, H., and Siegel, R.M. 2006. Homotypic FADD interactions through a conserved RXDLL motif are required for death receptor-induced apoptosis. *Cell Death Differ* **13**(10): 1641-1650.
- Niikura, T., Hashimoto, Y., Tajima, H., Ishizaka, M., Yamagishi, Y., Kawasumi, M., Nawa, M., Terashita, K., Aiso, S., and Nishimoto, I. 2003. A tripartite motif protein TRIM11 binds and destabilizes Humanin, a neuroprotective peptide against Alzheimer's disease-relevant insults. *Eur J Neurosci* **17**(6): 1150-1158.
- Nisole, S., Stoye, J.P., and Saib, A. 2005. TRIM family proteins: retroviral restriction and antiviral defence. *Nature reviews* **3**(10): 799-808.

- O'Shea, E.K., Klemm, J.D., Kim, P.S., and Alber, T. 1991. X-ray structure of the GCN4 leucine zipper, a two-stranded, parallel coiled coil. *Science* **254**(5031): 539-544.
- Ohlsson, M., Jonsson, R., and Brokstad, K.A. 2002. Subcellular redistribution and surface exposure of the Ro52, Ro60 and La48 autoantigens during apoptosis in human ductal epithelial cells: a possible mechanism in the pathogenesis of Sjogren's syndrome. *Scand J Immunol* **56**(5): 456-469.
- Osborn, S.L., Sohn, S.J., and Winoto, A. 2007. Constitutive phosphorylation mutation in Fas-associated death domain (FADD) results in early cell cycle defects. *The Journal of biological chemistry* **282**(31): 22786-22792.
- Roy, A., Hong, J.H., Lee, J.H., Lee, Y.T., Lee, B.J., and Kim, K.S. 2008. In vitro activation of procaspase-8 by forming the cytoplasmic component of the death-inducing signaling complex (cDISC). *Molecules and cells* **26**(2): 165-170.
- Sabile, A., Meyer, A.M., Wirbelauer, C., Hess, D., Kogel, U., Scheffner, M., and Krek, W. 2006. Regulation of p27 degradation and S-phase progression by Ro52 RING finger protein. *Molecular and cellular biology* **26**(16): 5994-6004.
- Sandu, C., Morisawa, G., Wegorzewska, I., Huang, T., Arechiga, A.F., Hill, J.M., Kim, T., Walsh, C.M., and Werner, M.H. 2006. FADD self-association is required for stable interaction with an activated death receptor. *Cell Death Differ* **13**(12): 2052-2061.
- Scaffidi, C., Krammer, P.H., and Peter, M.E. 1999. Isolation and analysis of components of CD95 (APO-1/Fas) death-inducing signaling complex. *Methods (San Diego, Calif)* **17**(4): 287-291.
- Strandberg, L., Ambrosi, A., Espinosa, A., Ottosson, L., Eloranta, M.L., Zhou, W., Elfving, A., Greenfield, E., Kuchroo, V.K., and Wahren-Herlenius, M. 2008. Interferon-alpha induces up-regulation and nuclear translocation of the Ro52 autoantigen as detected by a panel of novel Ro52-specific monoclonal antibodies. *J Clin Immunol* **28**(3): 220-231.
- Stremlau, M., Perron, M., Lee, M., Li, Y., Song, B., Javanbakht, H., Diaz-Griffero, F., Anderson, D.J., Sundquist, W.I., and Sodroski, J. 2006. Specific recognition and accelerated uncoating of retroviral capsids by the TRIM5alpha restriction factor. *Proc Natl Acad Sci U S A* **103**(14): 5514-5519.
- Takahata, M., Bohgaki, M., Tsukiyama, T., Kondo, T., Asaka, M., and Hatakeyama, S. 2008. Ro52 functionally interacts with IgG1 and regulates its quality control via the ERAD system. *Molecular immunology* **45**(7): 2045-2054.
- Wada, K. and Kamitani, T. 2006a. Autoantigen Ro52 is an E3 ubiquitin ligase. *Biochem Biophys Res Commun* **339**(1): 415-421.

- Wada, K. and Kamitani, T. 2006b. UnpEL/Usp4 is ubiquitinated by Ro52 and deubiquitinated by itself. *Biochem Biophys Res Commun* **342**(1): 253-258.
- Yang, K., Shi, H.X., Liu, X.Y., Shan, Y.F., Wei, B., Chen, S., and Wang, C. 2009. TRIM21 is essential to sustain IFN regulatory factor 3 activation during antiviral response. *J Immunol* **182**(6): 3782-3792.
- Yoshimi, R., Chang, T.H., Wang, H., Atsumi, T., Morse, H.C., 3rd, and Ozato, K. 2009. Gene disruption study reveals a nonredundant role for TRIM21/Ro52 in NF-kappaB-dependent cytokine expression in fibroblasts. *J Immunol* **182**(12): 7527-7538.
- Young, J.A., Sermwittayawong, D., Kim, H.J., Nandu, S., An, N., Erdjument-Bromage, H., Tempst, P., Coscoy, L., and Winoto, A. 2011. Fas-associated Death Domain (FADD) and the E3 Ubiquitin-Protein Ligase TRIM21 Interact to Negatively Regulate Virus-induced Interferon Production. *The Journal of biological chemistry* **286**(8): 6521-6531.
- Zhang, J., Cado, D., Chen, A., Kabra, N.H., and Winoto, A. 1998. Fas-mediated apoptosis and activation-induced T-cell proliferation are defective in mice lacking FADD/Mort1. *Nature* **392**(6673): 296-300.
- Zhang, J., Kabra, N.H., Cado, D., Kang, C., and Winoto, A. 2001. FADD-deficient T cells exhibit a disaccord in regulation of the cell cycle machinery. *The Journal of biological chemistry* **276**(32): 29815-29818.

Appendix A

ECONOMICAL METHOD FOR MIDIPREP PLASMID DNA PURIFICATION USING DIATOMACEOUS EARTH³

³ Modified from Sermwittayawong¹ D, Jakkawanpitak C, Waji N, Nongporn Hutadilok-Towatana N, ECONOMICAL METHOD FOR MIDIPREP PLASMID DNA PURIFICATION USING DIATOMACEOUS EARTH. Manuscript accepted.

Abstract

Plasmid is an important tool for this research and many other applications. Obtaining a high quality plasmid in a low cost is an important task for my laboratory. In this report, I describe an economical method for plasmid DNA purification from a 50 ml bacterial culture using diatomaceous earth (DE). Without using a vacuum system, this method of purification requires plastic pipette tips, conical tubes, and centrifuges. The resulting plasmids have a high yield from 200-800 μg with the A_{260}/A_{280} ratio from 1.8-2.0 and are suitable for DNA sequencing and transfection assay.

Introduction

The project: “Analysis of the Physical Interaction Between Fas–Associated Death Domain (FADD) and Tripartite Motif-Containing 21 (Trim21), an E3 Ubiquitin Ligase” requires several plasmids for transfection. Production of high quality plasmid DNA in the amount suitable for transfection assays is a necessary task. Commercial plasmid kits could be a solution for a high quality and yield plasmid, but the cost of purchasing purification kits could be substantial. To save the cost of plasmid purification, I have created homemade spun columns to use with diatomaceous earth (DE).

DE is among the best reagents for plasmid DNA purification for a high quality plasmid DNA. Methods for using DE have been described (Carter and Milton 1993; Parrish and Greenberg 1995; Machesky 1996; Kim et al. 2006). DE contains silica dioxide, which binds DNA in the presence of chaotropic salts such as guanidine hydrochloride, sodium iodide, and guanidine isothiocyanate (Vogelstein and Gillespie 1979). These chaotropic agents can also denature proteins. DNA that binds to the resin can be washed and eluted using hot water.

Aside from a low cost, the method presented here can be performed without using a vacuum system and commercial columns, which might not be accessible in some laboratories. With a 50 ml bacterial culture, my method of plasmid purification yields 200-800 μg plasmids. The plasmids are highly pure, with the A_{260} - A_{280} ratio from 1.8-2.0, and they can be used for DNA sequencing and transfection into tissue culture cells.

Materials and methods

Cell culture

A 50 ml bacterial culture was seeded from a single colony of *Escherichia coli* DH5 α strain harboring a desire plasmid DNA. The 2XTY medium in a 500 ml Erlenmeyer flask was supplemented with 100 μ g/ml Ampicillin. The culture flask was placed in an orbital shaker and incubated at 37°C, 220 rpm for 16-18 hours. After centrifugation, cell pellet could be kept at -20°C until the plasmid purification.

Alkaline lysis

The alkaline lysis method was modified from the previous protocols by Dr. Ravi Iyer⁴. Briefly, 5 ml solution 1 (25 mM Tris-Cl pH 8.0, 50 mM glucose, 10 mM EDTA, and 40 μ g/ml RNaseA) was used to resuspend cell pellet. After transferring to a clean 50-ml conical tube, 10 ml solution 2 (0.2 M NaOH and 1 % SDS) was added to break open cells, followed by gentle inversions and incubation at room temperature for 5 minutes. Then, 5 ml solution 3 (1.25 M potassium acetate and 1.25 M acetic acid) was subsequently added, mixed, and incubated on ice for 30 minutes. An addition of solution 3 caused a formation of white, fluffy precipitates, which were subsequently removed by filtration through a Whatman paper. The clear supernatant was transferred to a 35-ml screw-capped tube, followed by an addition of 0.6 volume isopropanol. After vigorous shakings, the sample was placed on ice for 5-10 minutes and subsequently centrifuged at 12,096 x g for 10 minutes to precipitate the DNA. After removal of supernatant, the DNA pellet could be stored at -20°C or proceeded to the next step.

Homemade column

⁴ (<http://iubio.bio.indiana.edu:7131/bionet/mm/methods/1993-November/009411.html>)

A spun column for plasmid DNA isolation was made of a 5-ml plastic pipette tip (for a P-5000 pipette), a 15-ml tube (Corning), and cotton. First, the narrow end of a plastic pipette tip was stuffed tightly with some cotton, which retains the resin during centrifugation (Figure 5A and 5B). Then, a spun column was created by inserting a stuffed tip in a 15-ml conical tube (Figure 5D).

Purification with diatomaceous earth (DE)

Purification procedures and the binding buffer were modified from the previous protocol (Machesky 1996). First, DNA in the isopropanol-precipitated pellet was resuspended with 1000 μ l Milli-Q water. Then, 5 ml binding buffer (7 M guanidine hydrochloride (GuHCl) in 50 mM Tris-Cl buffer pH 7.0 and 20 mM EDTA) was added. After adding 1.0 g DE (Sigma D5509), the mixture was rocked at a low speed at room temperature for 45-60 minutes. The resin slurry, which contained DNA, was then equally divided and transferred into 4 homemade spun columns for centrifugation in a swing-out centrifuge at 2,863 x g for 5 minutes. The flow-through was collected in a clean tube for troubleshooting. The resin, which was trapped in a column, was washed twice with 3 ml solution 4 (20 mM Tris-Cl pH. 7.5, 200 mM NaCl, 5 mM EDTA, and 50 % ethanol). Then, the columns were centrifuged at the same speed for another 10 minutes, or until the resin was completely dried. Prior to eluting the DNA, the 15-ml conical tube that support a column was changed to a clean one, which would be used for DNA collection. To elute the DNA, 250 μ l 72°C Milli-Q water was added to the resin, and the spun column was centrifuged at the same speed for 5 minutes. The elution was repeated once more and combined with the first elution. Thus, 4 homemade spun columns were used for one plasmid purification, which required a total of 2 ml elution solution. The eluted plasmid

could be directly used for many assays such as gel electrophoresis, restriction digestion, sequencing, and transfection assay. The A_{260} and A_{280} absorbances of the plasmids were determined using HP8453 UV-Visible Spectrophotometer.

Transfection assay

The pCI-HA_hIRF3 plasmid purified with this method was transfected into HEK293T cells (ATCC: CRL-11268) with Trans LT1 (Mirus), using the protocol described by the manufacturer's instruction. Cells were harvested 48 hours post-transfection and stored in a -80°C until needed.

Western blotting analysis

Soluble extract was produced by cell lysis against the lysis buffer (50 mM Tris-Cl pH 7.4, 150 mM NaCl, 1 mM EDTA, 0.5 % NP-40, 1x complete set protease inhibitors from Roche, 1 mM NaF, and 1 mM Na_3VO_4). The extract was then resolved by SDS-PAGE and transferred to a nitrocellulose membrane for Western blotting analysis using anti-HA tag (ABCAM). Incubations with the primary antibody (anti-HA tag, 1:4,000 diluted) and the secondary antibody (goat-anti rabbit HRP conjugated, 1:10,000 diluted) were performed for 2 hours at room temperature for each. SuperSignal West Pico Chemiluminescent Substrate (Pierce) was used prior to X-ray film exposure. The film was developed with an X-ray film-processing machine.

Results

Creating a homemade spun column

A spun column for plasmid DNA isolation was made of a 5-ml plastic pipette tip (for a P-5000 pipette), a 15-ml tube (Corning), and cotton (Figure 5). With a type of 5-ml plastic tip we used, a 15-ml conical tube from Corning gives the best fit. Any brand of 15-ml tube could probably be used, as long as the stuffed tip could be removed from the tube after centrifugation. In addition, the 3 ml dead volume in the column is required because it is used as a reservoir for liquid resulted from centrifugation (Figure 5D).

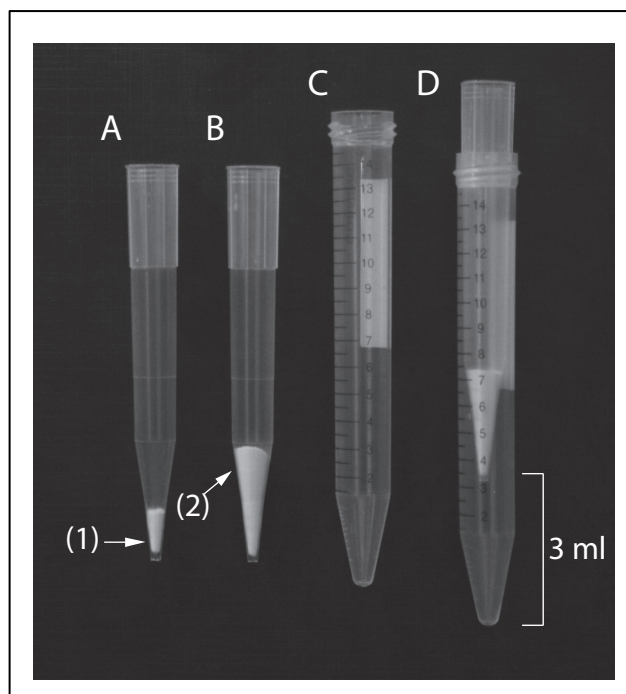


Figure 5: Homemade spun column. A) A 5-ml plastic pipette tip stuffed with some cotton (1); B) A stuffed tip in A filled with diatomaceous earth or DE (2); C) a 15-ml conical tube; D) a homemade spun column is made from a stuffed tip in B) and a tube C). Notice that after fitting the tip, there is a 3-ml dead space volume, which serves as a reservoir for liquid collection.

To find the right amount of DE used for each column, the amount of DE per column were varied from 0.2-0.5 g, whereas the elution solution was kept constant at 250

μl for each elution round. Percent recovery was calculated from the amount of plasmid DNA eluted from the column and the amount of total plasmid DNA before purification with DE. Results in Figure 6 show that the best amount of resin was 0.25 g/column, whereas the higher amount of resin decreased the percent recovery of the plasmid DNA. The decrease of the plasmid yield as the amount of the resin increased probably because some of the DNA was still bound to the resin. To test this idea, additional elutions were applied with 0.4 and 0.5 g DE/column. The results show that 30%-40% plasmid DNA could be eluted from the resin (data not shown). Thus, more elution solution is required to obtain more plasmid DNA. However, increasing the elution volume would also dilute the overall DNA concentration. Together, the amount of DE at 0.25 g/column or 1.0 g for one plasmid purification is the best amount of resin for the highest percent recovery.

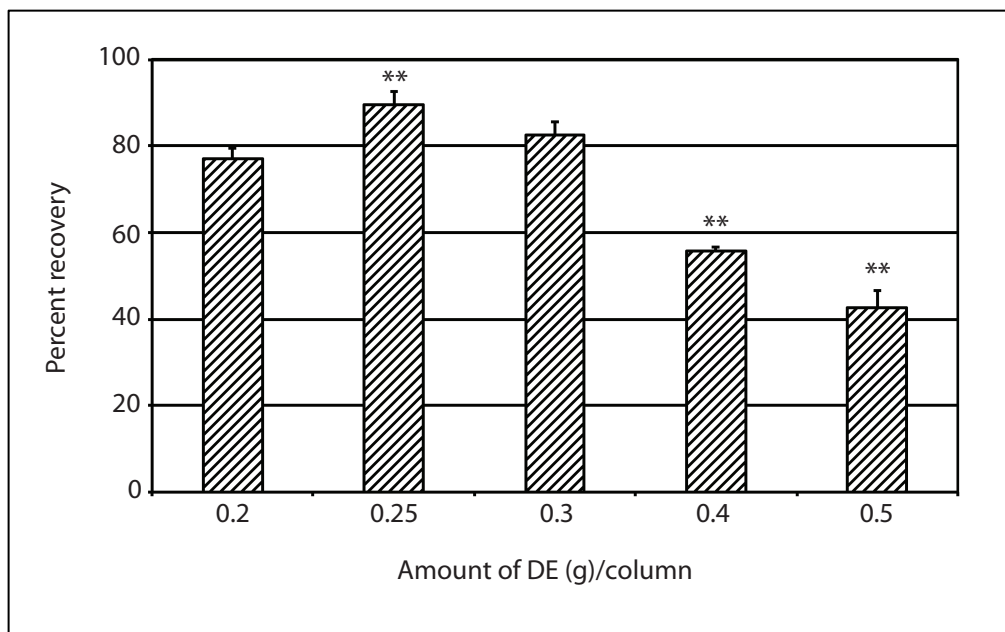


Figure 6: Percent recovery of the plasmid from different amount of DE. For each experiment, the DNA pellet was dissolved with water and split into two sets: one for purification with DE and the other for determining the total amount of plasmids. Thus, percent recovery was calculated as a percent of the plasmid purified with DE in comparison with the total amount of plasmid without DE purification. Data presented are the averages (\pm standard deviation) of three independent experiments. One and two asterisks indicate significant differences ($P < 0.05$) and ($P < 0.01$), respectively from the 0.2 g DE/column, based on Student's *t* test.

Room temperature water is as good as hot water

Because the elution solutions described in literature were either hot water or Tris-EDTA buffer pH 8.0 (Carter and Milton 1993; Kim et al. 2006), it remains questionable whether these would be the best elution solutions. Therefore, 4 different elution solutions: hot Milli-Q water at 72°C, room temperature Milli-Q water, ice-cold Milli-Q water, and 10 mM Tris-Cl pH 8.0 were used to test their elution efficiency. The results show that both hot and room temperature water gave a comparable plasmid yield (Figure 7). Interestingly, 10 mM Tris-Cl pH 8.0 was found to be the worst elution solution for this protocol.

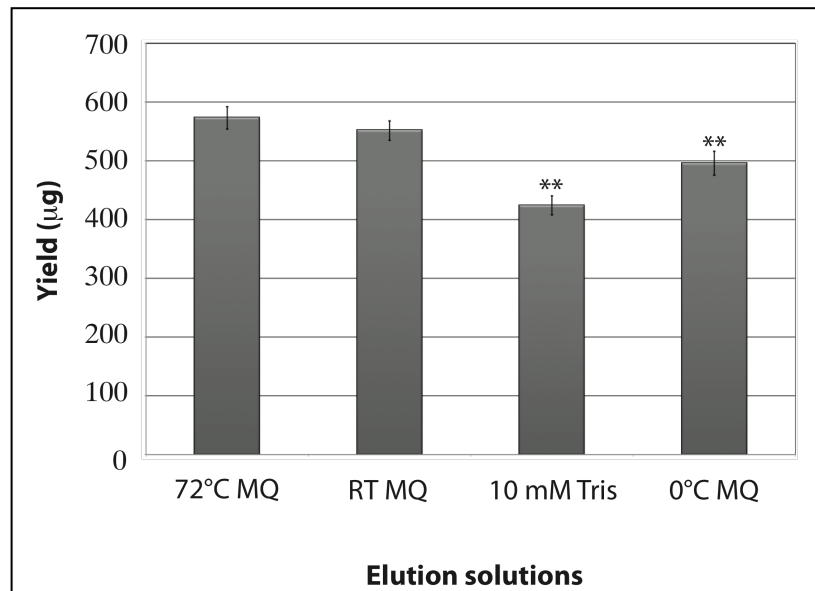


Figure 7: Hot water is the best solution to elute plasmids from the resin. Isopropanol-precipitated pcDNA3 plasmid from a 50 ml culture was equally divided into 4 columns for 4 different elution solutions: 72°C Milli-Q water, 10 mM Tris-Cl pH 8.0, room temperature, and ice-chilled Milli-Q water. MQ is abbreviated for Milli-Q. Data bars are the averages (\pm standard deviation) of three independent experiments. The two asterisks indicate a significant difference ($P < 0.01$) from the reference condition (72°C MQ water), based on Student's *t* test.

Applications of the plasmid DNA

Gel electrophoresis of purified plasmids shows that all plasmids were fractionated into two bands which are normally found in plasmid DNA (Willshaw et al. 1979). The first one is a fast migrating band (supercoiled or covalently closed circular plasmid (CCC), whereas the slower migrating band represents an open circular form of plasmid (Figure 8A). All purified plasmids have an A_{260}/A_{280} ratio within the range of 1.8-2.0 (Table 4) and can be used for transfection assay or DNA sequencing (Figure 8B and data not shown).

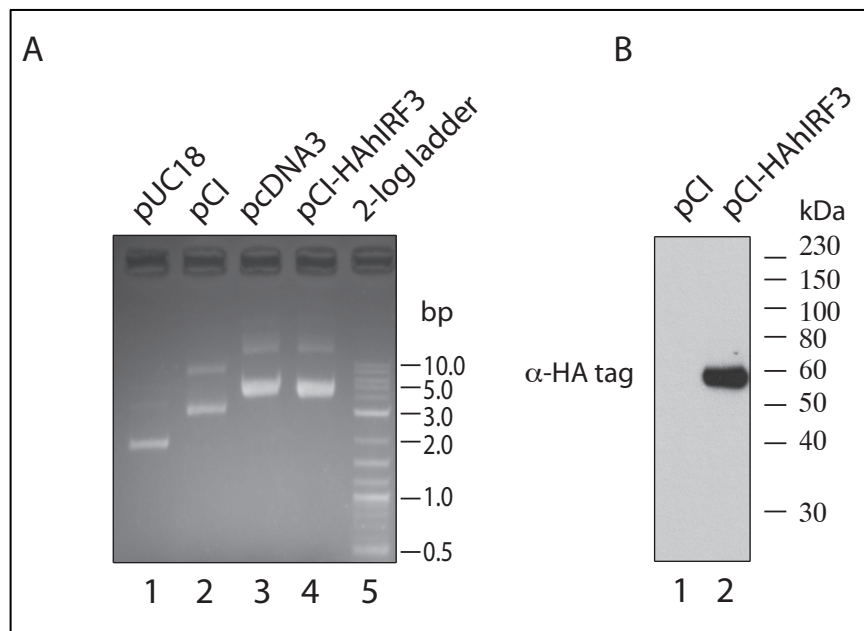


Figure 8: Analysis of purified plasmids with agarose gel electrophoresis and transfection assay A) Ethidium bromide stained agarose gel show four different plasmids purified with this method. Top and bottom bands on each lane represent open circular and supercoiled plasmids, respectively. B) Purified plasmids from this protocol are suitable for transfection assays. Purified pCI-HAhIRF3 plasmid was transfected into the HEK293T cells, using LT1 (Mirus). Expression of HA-tagged hIRF3 was analyzed by Western blotting, using anti-HA tag polyclonal antibodies (ABCAM).

Table 4: Absorbances of plasmids purified with this technique.

Name	Purification #	Dilution	Abs<260nm>	Abs<280nm>	Ratio (A_{260}/A_{280})
pCI-HAhIRF3	1	20.00	0.617	0.323	1.912
pCI-HAhIRF3	2	20.00	0.559	0.293	1.910
pCI-HAhIRF3	3	20.00	0.595	0.307	1.940
pcDNA3	1	20.00	0.590	0.308	1.916
pcDNA3	2	20.00	0.558	0.293	1.905
pcDNA3	3	20.00	0.603	0.315	1.913
pCI	1	20.00	0.441	0.220	2.004
pCI	2	20.00	0.408	0.222	1.838
pCI	3	20.00	0.375	0.196	1.914
pUC18	1	20.00	0.165	0.088	1.875
pUC18	2	20.00	0.180	0.095	1.895
pUC18	3	20.00	0.120	0.063	1.904
pCI-hTrim21	1	20.00	0.508	0.273	1.861
pCI-hTrim21	2	20.00	0.645	0.342	1.886
pCI-hTrim21	3	20.00	0.615	0.331	1.858
pCI-hTrim21	4	20.00	0.524	0.284	1.845
pCI-hFaddHisFlag	1	30.00	0.316	0.174	1.816
pCI-hFaddHisFlag	2	30.00	0.308	0.169	1.822
pCI-hFaddHisFlag	3	30.00	0.255	0.138	1.848
pCI-hFaddHisFlag	4	30.00	0.312	0.165	1.891
pCI-HAhTrim39	1	15.00	0.444	0.243	1.827

Table 5: Comparing Qiagen plus midi kit and the homemade spun column

Feature	Qiagen Plasmid Plus Midi Kit	Homemade Spun column
Total purification time	30-45 minutes	2-4 hours
Culture scale	25-35 ml	50 ml
Expected yield for a high-copy plasmid	150-250 μg^5	200-800 μg^6
A_{260}/A_{280}	1.8-2.0	1.8-2.0
DNA contamination	No contamination	No contamination
Processing	manual (centrifugation and vacuum), parallel processing	Centrifugation

Table 6: Comparing the cost of purification kits and the homemade spun column

Brand	Size (number of purifications)	Price ⁷	Cost for one purification
Qiagen: Plasmid Plus Midi Kit	100	\$1,094	\$10.94
Roche: Genopure Plasmid Midi Kit	20	\$185	\$9.25
BioRad: Quantum Prep Plasmid Midiprep Kit	20	\$175	\$8.75
E.Z.N.A.: Plasmid Midi Kit	100	\$504	\$5.04
Homemade spun column	-	-	Less than \$1

⁵ Data taken from the technical specification at www.qiagen.com, not from experiments

⁶ Yield depends on the size and the origin of replication of the plasmids

⁷ Price shown on the manufacturer's website. Accessed Oct 30th, 2013

Discussion

This DNA purification technique using homemade spun column and DE produces plasmids in a high quality that can be used in many applications. I found that the yield from this purification was varied from 200-800 µg, depending upon the size and the origin of replication of the plasmid (data not shown). Although this purification technique confers a much higher yield than a commercial kit (Table 5), the filtration step after adding solution 3 takes almost one hour, which gives the total purification time of approximately 2-4 hours. However, I found that this filtration step removed many impurities, which may interfere with the subsequent purification with the DE (data not shown). In addition to the time, only a certain swing-out centrifuge can support the homemade spun column because of the long length of the spun column. Regardless of these disadvantages, this protocol does not require commercial plastic columns, a vacuum pump, and a vacuum manifold, making this protocol accessible for most laboratories. Assuming the major costs of the plasmid purification came from GuHCl (Sigma 50950, 1 kg), diatomaceous earth (Sigma D5509, 1 kg), isopropanol (LabScan, 4 l), and absolute ethanol (Macron, 2.5 l), the cost for one plasmid purification is estimated 26.70⁸ baht or less than \$1, which is at least 5 times cheaper than many commercial kits (Table 6), making this plasmid purification protocol relatively inexpensive and affordable.

⁸ Calculated based on the cost of each reagent purchased in Thailand. Vat 7% is included.

References

- Carter, M.J. and Milton, I.D. 1993. An inexpensive and simple method for DNA purifications on silica particles. *Nucleic Acids Res* **21**(4): 1044.
- Kim, T.H., Hwang, M.S., Song, J.-D., Oh, M.-H., Moon, Y.-H., Chung, I.K., Rhew, T.-H., and Lee, C.H. 2006. A Simple Method for Extraction of High Molecular Weight DNA from *Porphyra Tenera* (Rhodophyta) Using Diatomaceous Earth. *Algae* **21**: 261-266.
- Machesky, L. 1996. Plasmid Preparations with Diatomaceous Earth. in *Basic DNA and RNA Protocols* (ed. A. Harwood), pp. 269-272. Humana Press.
- Parrish, K.D. and Greenberg, E.P. 1995. A rapid method for extraction and purification of DNA from dental plaque. *Appl Environ Microbiol* **61**(11): 4120-4123.
- Vogelstein, B. and Gillespie, D. 1979. Preparative and analytical purification of DNA from agarose. *Proc Natl Acad Sci U S A* **76**(2): 615-619.
- Willshaw, G.A., Smith, H.R., and Anderson, E.S. 1979. Application of agarose gel electrophoresis to the characterization of plasmid DNA in drug-resistant enterobacteria. *J Gen Microbiol* **114**(1): 15-25.